

**ORIGINAL
RESEARCH**

T. Noguchi
T. Yoshiura
A. Hiwatashi
O. Togao
K. Yamashita
E. Nagao
T. Shono
M. Mizoguchi
S. Nagata
T. Sasaki
S.O. Suzuki
T. Iwaki
K. Kobayashi
F. Mihara
H. Honda

Perfusion Imaging of Brain Tumors Using Arterial Spin-Labeling: Correlation with Histopathologic Vascular Density

BACKGROUND AND PURPOSE: We investigated the relationship between tumor blood-flow measurement based on perfusion imaging by arterial spin-labeling (ASL-PI) and histopathologic findings in brain tumors.

MATERIALS AND METHODS: We used ASL-PI to examine 35 patients with brain tumors, including 11 gliomas, 9 meningiomas, 9 schwannomas, 1 diffuse large B-cell lymphoma, 4 hemangioblastomas, and 1 metastatic brain tumor. As an index of tumor perfusion, the relative signal intensity (SI) of each tumor (%Signal intensity) was determined as a percentage of the maximal SI within the tumor per averaged SI within normal cerebral gray matter on ASL-PI. Relative vascular attenuation (%Vessel) was determined as the total microvessel area per the entire tissue area on CD-34-immunostained histopathologic specimens. MIB1 indices of gliomas were also calculated. The differences in %Signal intensity among different histopathologic types and between high- and low-grade gliomas were compared. In addition, the correlations between %Signal intensity and %Vessel or MIB1 index were evaluated in gliomas.

RESULTS: Statistically significant differences in %Signal intensity were observed between hemangioblastomas versus gliomas ($P < .005$), meningiomas ($P < .05$), and schwannomas ($P < .005$). Among gliomas, %Signal intensity was significantly higher for high-grade than for low-grade tumors ($P < .05$). Correlation analyses revealed significant positive correlations between %Signal intensity and %Vessel in 35 patients, including all 6 histopathologic types ($r_s = 0.782$, $P < .00005$) and in gliomas ($r_s = 0.773$, $P < .05$). In addition, in gliomas, %Signal intensity and MIB1 index were significantly positively correlated ($r_s = 0.700$, $P < .05$).

CONCLUSION: ASL-PI may predict histopathologic vascular densities of brain tumors and may be useful in distinguishing between high- and low-grade gliomas and in differentiating hemangioblastomas from other brain tumors.

Arterial spin-labeling perfusion imaging (ASL-PI) is an MR imaging technique for perfusion measurement. This unique technique requires no extrinsic tracer, such as gadolinium chelates or radionuclides. Instead, it uses electromagnetically labeled arterial blood water as a freely diffusible intrinsic tracer. In clinical applications, this technique has proved reliable and reproducible in the assessment of cerebral blood flow (CBF) in various pathologic states, including cerebrovascular disease,¹⁻³ neurodegenerative disease,^{4,5} and temporal lobe epilepsy.^{6,7}

Some clinical studies have reported the clinical usability in differential diagnosis as well as the therapeutic efficacy of the brain tumor based on tumor blood flow (TBF) measured by ASL-PI.⁸⁻¹³ However, the relationship between ASL-PI and histopathologic findings has not been sufficiently understood. The purpose of our study was to compare ASL-PI to histopathologic findings in brain tumors.

Materials and Methods

Patient Population

In 2005 and 2006, 40 patients with brain tumors underwent ASL-PI at Kyushu University Hospital. Three patients with recurrent tumors (1 glioblastoma, 1 anaplastic oligodendroglioma, and 1 dysembryoplastic neuroepithelial tumor [DNT]) were excluded from this study because they had already undergone surgery, radiation therapy, or chemotherapy. One patient with a metastatic tumor diagnosed by cytology was excluded because of the absence of a histologic specimen. One patient with a pleomorphic xanthoastrocytoma was excluded because the tumor cells as well as the vascular endothelial cells were immunostained for CD-34 and the histopathologic vascular attenuation was impossible to measure accurately. The remaining 35 patients (13 men and 22 women; age range, 4–76 years; median age, 50.7 years) were included in our study. Histologic diagnoses of the tumors according to the World Health Organization (WHO) brain tumor classification revised in 2007¹⁴ included 11 gliomas (5 glioblastomas [WHO grade IV], 1 anaplastic oligodendroglioma [III], 1 gliomatosis cerebri [III], 3 diffuse astrocytomas [II], and 1 DNT [I]), 9 meningiomas (6 meningiomas of WHO grade I, 2 atypical meningiomas, and 1 papillary meningioma), 9 schwannomas, 1 diffuse large B-cell lymphoma, 4 hemangioblastomas, and 1 metastatic brain tumor. Written informed consent was obtained from each patient or the patient's parent with the approval of the institutional review board. The histologic specimen was obtained by partial or total surgical resection in 32 patients, open biopsy in 2 patients, and stereotactic biopsy in 1 patient.

Received August 21, 2007; accepted after revision October 15.

From the Departments of Clinical Radiology (T.N., T.Y., A.H., O.T., K.Y., E.N., F.M., H.H.), Neurosurgery (T.S., M.M., S.N., T.S.), and Neuropathology (S.O.S., T.I.), Graduate School of Medical Sciences, Kyushu University, Fukuoka, Japan; and the Radiological Center (K.K.), Kyushu University Hospital, Fukuoka, Japan.

This work was supported by a Grant-in-Aid for Scientific Research from the Japan Society for the Promotion of Science.

Please address correspondence to Tomoyuki Noguchi, MD, Department of Clinical Radiology, Kyushu University, 3-1-1, Maidashi, Higashi-ku, Fukuoka PRF, Japan 812-8582; e-mail: tnogucci@radiol.med.kyushu-u.ac.jp

DOI 10.3174/ajnr.A0903

MR Imaging

All ASL-PI examinations were performed on a clinical 1.5T MR imaging unit (Magnetom Symphony; Siemens, Erlangen, Germany) with a product transmit/receive head coil within 0–40 days before surgery. ASL-PI was performed by using a second version of quantitative imaging of perfusion by means of a single subtraction with the addition of thin-section periodic saturation (Q2TIPS), which is a pulsed arterial spin-labeling method that enables the acquisition of multiple sections.¹⁵ Q2TIPS has 2 important planes and 3 parameters: a labeling plane; an imaging plane; and T11, T11S, and T12.¹⁵ The labeling plane is the region where the proximal arterial blood is labeled by an inversion recovery radio-frequency pulse. The imaging plane is the region where the data acquisition of the perfusion imaging is performed. T11 is a timing parameter representing the amount of time that passes between the inversion recovery pulse for labeling the blood and the periodic saturation pulse, both of which are applied to the labeling plane. Therefore, T11 is related to the amount of labeled blood volume. T11S is a timing parameter and represents the amount of time between the inversion recovery pulse for labeling and the end of the saturation pulse on the labeling plane. T12 is a timing parameter and represents the amount of time between the inversion recovery pulse for labeling and the beginning of the imaging data acquisition by an echo-planar imaging (EPI) sequence. Under the current Q2TIPS setting, the labeling plane comprised a 100-mm-wide region and was placed 10 mm proximal to the imaging plane. The imaging plane was set so as to coincide with the greatest dimension of the tumor by reference to the findings on T1-weighted images (T1WI), T2-weighted images (T2WI), and fluid-attenuated inversion recovery images (FLAIR).

Five imaging sections were acquired sequentially in a proximal-to-distal direction by using a single-shot gradient-echo EPI technique (section width/gap = 5/2.5 mm, TR/TE = 2100/26 ms, FOV = 240 × 240 mm, matrix = 64 × 64 pixels, voxel size = 3.75 × 3.75 × 5 mm, band width = 1532 Hz/pixel, crusher gradients = 10 cm/s, phase partial Fourier acquisition rate = 6/8, phase oversampling = 13%, acquisition time per section = 49.5 ms). The signal intensity of the perfusion images was corrected for the delay due to the sequential acquisition. The inversion and saturation pulse parameters of Q2TIPS were set as follows: T11 = 900 ms, T11S = 1300 ms, and T12 = 1400 ms. Fifty pairs of labeled and nonlabeled images were obtained in 3 minutes 30 seconds. The perfusion images were generated by subtracting the labeled image from the nonlabeled image at each section position.

In addition to ASL-PI, conventional images including T1WI, T2WI, FLAIR, and postcontrast T1WI were obtained by using any of 3 different clinical 1.5T MR imaging units (Magnetom Vision and Symphony, Siemens; Achieva, Royal Philips Electronics, Eindhoven, the Netherlands). The parameters for those conventional images were as follows: T1WI: TR/TE = 441–620/9.5–14 ms; T2WI: TR/TE = 2500–4902.5/90–100 ms; FLAIR: TR/TE/ TI = 9000/97–110/2200–2400 ms; postcontrast T1WI: TR/TE = 525–800/17 ms. Postcontrast images were obtained after intravenous administration of gadolinium diethylene triamine pentaacetic acid (0.1 mmol/kg; Magnevist, Nihon Schering, Osaka, Japan). In 1 patient, postcontrast T1WI was not performed because the patient had asthma.

ASL Data Processing

By reference to the findings on T1WI, T2WI, FLAIR, and postcontrast T1WI, a region of interest that had a size of at least 26 pixels was placed within the tumor. Additionally, on the same image, another region of interest was placed within the normal-appearing cortical gray matter

(GM) in the contralateral cerebral hemisphere on a simply visual basis. Each region of interest was set by a neuroradiologist (T.N.) who was not blinded to the diagnosis. As an index of tumor perfusion, we used a relative signal intensity (SI) (%Signal intensity), which was defined as the ratio of maximal SI within the tumor (Tmax) to the averaged SI of GM (GMav) (%Signal intensity = Tmax / GMav × 100[%]). The relative perfusion index was used rather than the absolute blood-flow value because the accuracy of the absolute perfusion measurement by using Q2TIPS has not been fully established, especially in pathologic conditions.^{8,9} Although the absolute blood flow value could be theoretically determined by using ASL,^{15,16} the quantitative CBF by using the ASL sequence can be affected by unstable factors such as the arterial transit time of the labeled blood from the labeling plane to the brain tissue within the imaging plane, the local relaxation times of tissue and blood, the assumption of a constant T1 relaxation time of arterial blood irrespective of vessel size or blood oxygenation,¹⁰ and the equilibrium magnetization and T1 value of the blood.¹⁷ CBF values measured by using ASL are thought to be proportional rather than equivalent to the actual regional CBF values.^{8,9}

Additionally, considering the large interindividual differences in perfusion,¹⁸ the relative perfusion measurement is the most reliable method at present. The averaged SI of GM instead of that of white matter (WM) was adopted as a reference of relative perfusion because the arterial transit time of WM was much longer than that of GM, resulting in a substantial underestimation of the blood flow for WM.^{19,20} The maximal SI rather than the averaged SI of brain tumors was adopted as a parameter for relative perfusion to detect the most vascularized portion of the tumor, which may correspond to the highest grade region.¹¹

Histopathologic Evaluations

We examined the vascular attenuation and the cell proliferation as the histopathologic parameters of the tumors.

To evaluate the vascular attenuation of the brain tumors, we immunostained the tissue sections for CD-34 (Novocastra Laboratories, Newcastle, UK), which identifies vascular endothelial cells. A microscopic field of the most intense vascularization in each specimen under a ×20 objective field (area = 0.33 mm²) was photographed as a JPEG file (1600 × 1200 pixels, 16.7 million colors, 8-bit) with a microscope digital color camera (Microscope Digital Camera DP20; Olympus, Tokyo, Japan). For each tumor, the relative vascular attenuation (%Vessel) was defined as the total area of vessel lumina surrounded by the endothelial cell layer as a percentage of the entire tissue area. The vessel lumina were recognized as an area surrounded by the CD-34–positive endothelial cell layer. On the image, the vessel area was distinguished by color by using Photoshop CS2 (Adobe Systems, San Jose, Calif). The tissue area was extracted by excluding the tissue-free space on the image by using Adobe Photoshop CS2. The image was analyzed with Image ALPHA 4.0.3.2 (Scion, Frederick, Md) to measure %Vessel by counting the pixel number of the total vessel lumina and that of the entire tissue.^{9,21–23}

To assess the proliferative activities of tumor cells, we immunostained glioma tissue sections with MIB1 (Dako, Glostrup, Denmark), a monoclonal antibody against Ki-67 antigen that is expressed throughout the cell cycle except at the G0 stage.^{24–26} The MIB1 index was measured in the microscopic area that showed the greatest number of immunopositive nuclei under a ×20 objective as a JPEG file with the microscope digital color camera by using the same conditions as previously described. MIB1 index was calculated as the percentage of the positive nuclei area divided by the whole nuclei area by

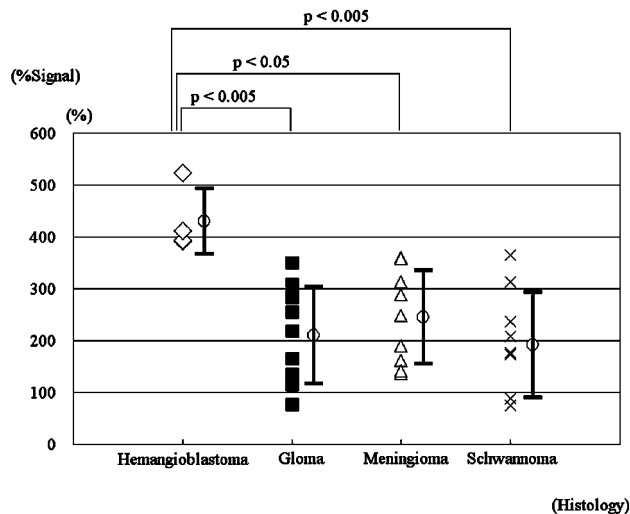


Fig 1. Relative maximal %Signal intensity in 4 histopathologic types of brain tumors. Statistically significant differences between hemangioblastomas and gliomas ($P < .005$), and meningiomas ($P < .05$) and schwannomas ($P < .005$) are revealed (Kruskal-Wallis test with Scheffé post hoc analysis).

using free computer software (Gunma-LI, Version 017; Gunma University, Gunma, Japan; available at <http://omt.med.gunma-u.ac.jp/~tgaku/GunmaLI>).

Data Analysis

%Signal intensity among the 4 histopathologic types including hemangioblastomas, gliomas, meningiomas, and schwannomas were compared by using the Kruskal-Wallis test with a Scheffé post hoc analysis under a significance level of .05.

The correlations between %Signal intensity and %Vessel were examined for 35 tumors, including all 6 histopathologic types, as well as for each of the 4 histopathologic types (ie, hemangioblastomas, gliomas, meningiomas, schwannomas). The correlations were then evaluated by using single linear regression analysis and Spearman signed rank test. P values under the level of .05 after application of the Bonferroni adjustment for multiple comparisons (5 comparisons) were considered statistically significant.

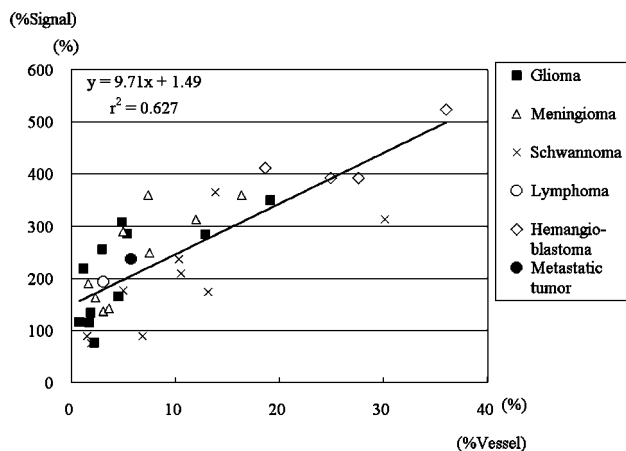


Fig 2. Scatter chart of %Signal intensity determined by ASL-PI and the %Vessel determined by histopathologic examination with regression lines in 35 tumors of 6 histopathologic types and 11 gliomas. Note the positive correlations between %Signal intensity and %Vessel in 35 cases ($\{x: \%Signal\ intensity; y: \%Vessel\}$, $y = 9.71x + 1.49$, $r^2 = 0.627$; $r_s = 0.782$, $P < .00005$) and in gliomas ($y = 1.16x + 1.49$, $r^2 = 0.514$; $r_s = 0.773$, $P < .05$).

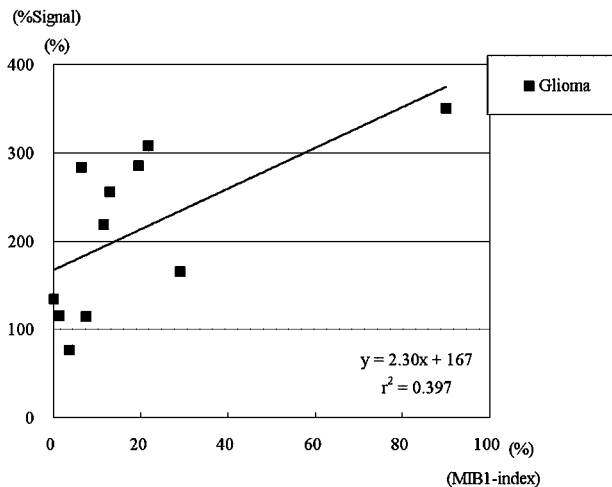


Fig 3. Scatter chart of %Signal intensity determined by ASL-PI and MIB1 index determined by histopathologic examination with a regression line in 12 gliomas. Note the positive correlation between %Signal intensity and MIB1 index in gliomas ($\{x: \%Signal\ intensity; y: \%Vessel\}$, $y = 2.30x + 1.67$, $r^2 = 0.397$; $r_s = 0.700$, $P < .05$).

In gliomas, the cell-proliferation potency estimated by the MIB1 index is closely related to the histologic grade.²⁷ We thus examined the correlation between %Signal intensity and the MIB1 index of gliomas by using single linear regression analysis and the Spearman signed rank test under the significance level of .05.

ASL-PI is reportedly useful for differentiating between high-grade (WHO grade III or IV) versus low-grade (I or II) gliomas.⁹⁻¹² We examined the difference in %Signal intensity between high- and low-grade gliomas by using Mann-Whitney U test under the significance level of .05.

Results

Figure 1 shows the differences in %Signal intensity among hemangioblastomas, gliomas, meningiomas, and schwannomas. There were statistically significant differences in %Signal intensity between hemangioblastomas on the one hand and, on the other, gliomas ($P < .005$), meningiomas ($P < .05$), and schwannomas ($P < .005$). No statistically significant difference was observed between any other combinations.

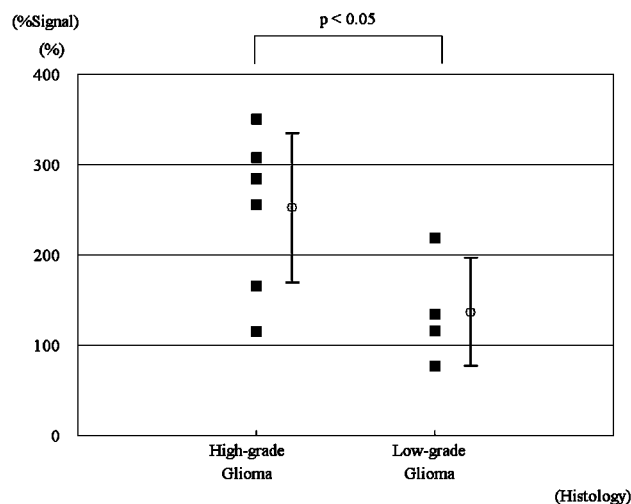


Fig 4. The relative maximal %Signal intensity in high- and low-grade gliomas. Note the significant difference between high- and low-grade gliomas ($P < .05$).

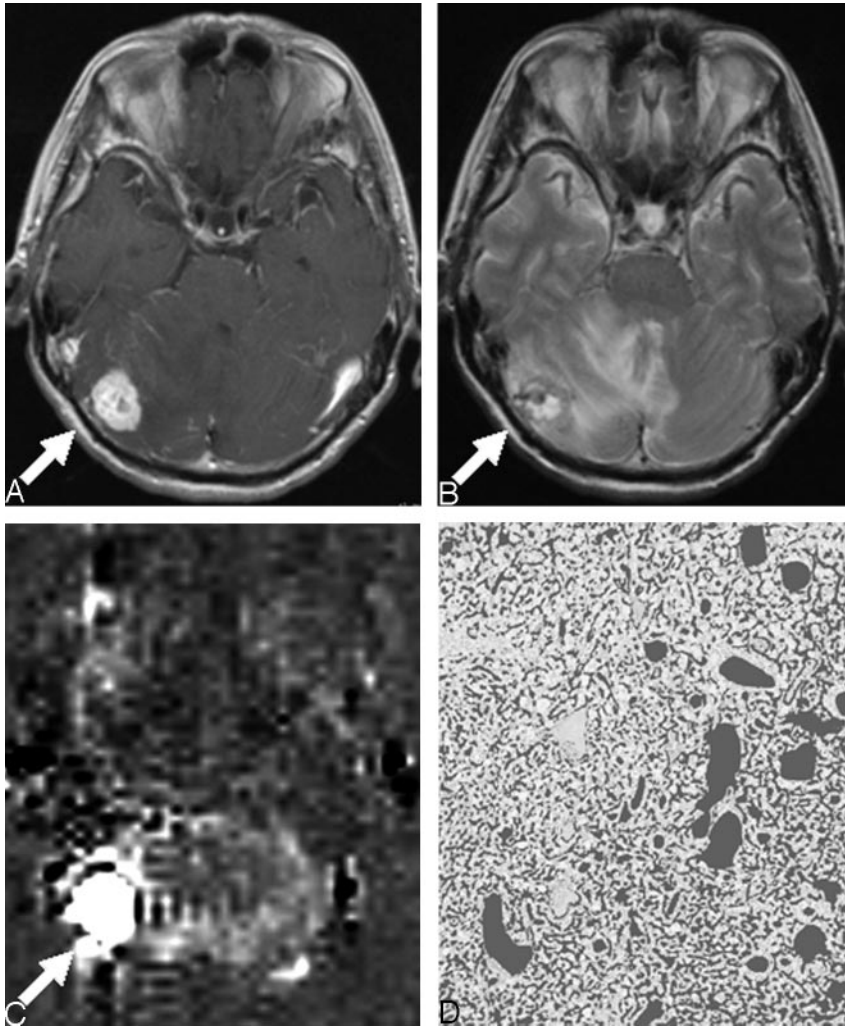


Fig 5. A 61-year-old woman with hemangioblastoma; post-contrast T1WI (TR/TE = 525/17 ms) (A), T2WI (2500/15 ms) (B), perfusion image by ASL (C), and CD-34-immunostained histopathologic specimen with the dark gray color overlaid on vessel lumen areas ($\times 20$) (D). A, Postcontrast T1WI shows a strongly enhanced mass (arrow) in the right cerebellar hemisphere. B, T2WI shows a high-signal-intensity mass (arrow) with surrounding edema. C, Perfusion image by ASL shows remarkably high signal intensity (%Signal intensity = 524%) (arrow). D, The image analysis of the CD-34-immunostained histopathologic specimen shows attenuated vascular proliferation (%Vessel = 36.0%).

Figure 2 shows the correlations between %Signal intensity and %Vessel. There were positive correlations between %Signal intensity and %Vessel in the 35 cases ($\{x: \%Signal\ intensity, y: \%Vessel\}$, $y = 9.72x + 1.49, r^2 = 0.627; rs = 0.782, P < .00005$) (Fig 2) and in gliomas ($y = 11.6x + 1.49, r^2 = 0.514; rs = 0.773, P < .05$). Correlations in hemangioblastomas ($rs = 0.200$), meningiomas ($rs = 0.717$), and schwannomas ($rs = 0.817$) did not reach statistical significance due to the small sample sizes, though there were trends toward positive correlations in the latter 2 tumor types.

Figure 3 shows the correlation between %Signal intensity and MIB1 index in gliomas. There was a positive correlation between %Signal intensity and MIB1 index in gliomas ($y = 2.30x + 1.67, r^2 = 0.397; rs = 0.700, P < .05$).

Figure 4 shows the difference in %Signal intensity between high-grade and low-grade gliomas. High-grade gliomas showed significantly higher %Signal intensity than low-grade gliomas ($P < .05$).

Figures 5 and 6 show representative cases of a hemangioblastoma and a glioblastoma, respectively.

Discussion

In previous reports, ASL-PI has been found useful in differentiating between high- and low-grade gliomas⁹⁻¹²; distinguishing glioblastomas from metastases, CNS lymphomas, and all

other glioma grades⁹; and predicting the outcome of metastatic brain tumor after radiosurgery.⁸ In our study, we recruited patients with brain tumors of various relatively common histologic types, including glioma, meningioma, schwannoma, malignant lymphoma, hemangioblastoma, and metastatic brain tumor and compared the TBF among them. We found that the %Signal intensity of the hemangioblastomas was significantly higher than that of the other 3 types of the brain tumors (gliomas, meningiomas, and schwannomas) (Fig 1), indicating that hemangioblastoma had the highest TBF. Histopathologically, hemangioblastoma is characterized by channels of thin-walled tightly packed blood vessels, varying in size and interspersed by polygonal lipid-laden stromal cells.²⁸ Our result may reflect high TBF through the abundant vessel network. This finding might be of use in differentiating hemangioblastomas from brain tumors in the posterior fossa. However, we did not compare hemangioblastoma versus metastases on the posterior fossa. Toward this end, additional examinations are desirable.

We found a positive correlation between %Signal intensity and %Vessel in the 35 patients. This may suggest that ASL-PI reflects the histopathologic vascularity across different types of brain tumors. We assume that the lack of a significant correlation in hemangioblastomas, meningiomas, and schwannomas was due to the small number of patients.

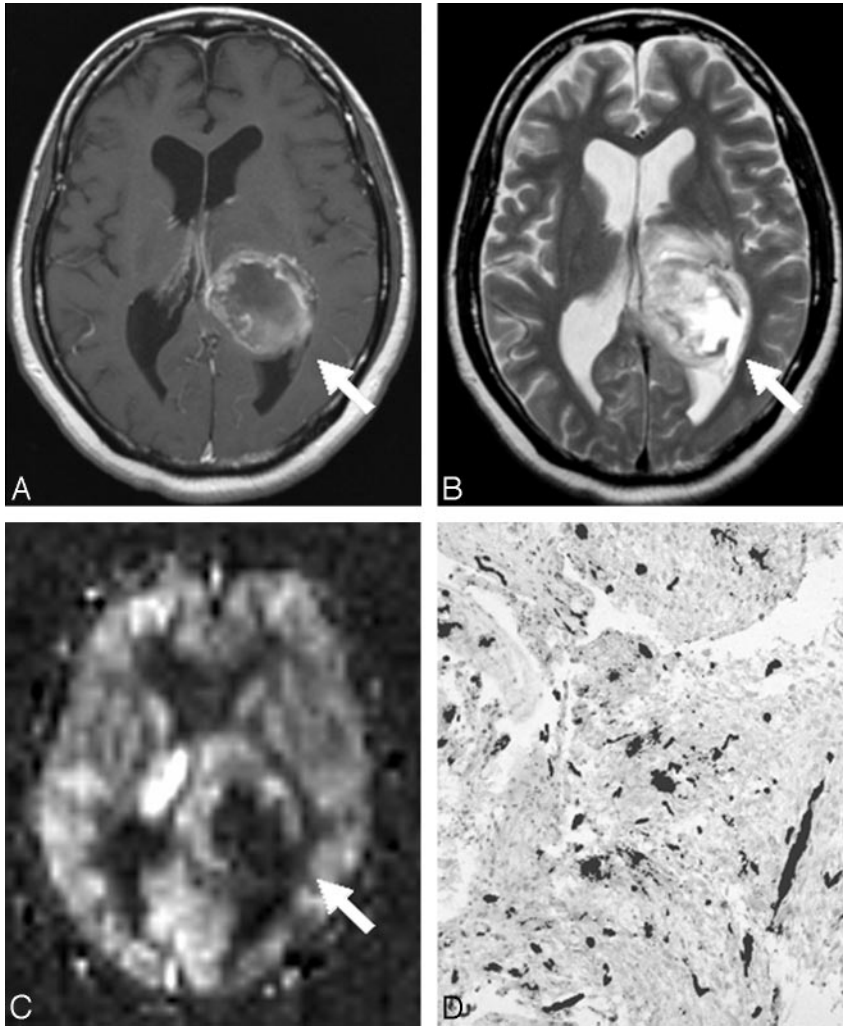


Fig 6. A 44-year-old woman with glioblastoma; postcontrast T1WI (591/17 ms) (A), T2WI (2800/93 ms) (B), perfusion image by ASL (C), and CD-34-immunostained histopathologic specimen with the dark gray color overlaid on vessel lumen areas ($\times 20$) (D). A, Postcontrast T1WI reveals a ringlike enhancing mass (arrow) in the left cerebral hemisphere. B, T2WI shows the high-intensity mass (arrow) with peritumoral edema. C, On the perfusion image by ASL, the tumor was depicted as a high-intensity area (%Signal intensity = 265%) with a central low perfusion area (arrow). Image analysis of the CD-34-immunostained histopathologic specimen shows scattered vascular proliferation (%Vessel = 2.97%).

There have been only a few reports regarding the correlation between ASL-PI and the histopathologic findings in brain tumors.^{9,13} Kimura et al¹³ reported a significant correlation in meningiomas between the relative mean TBF and the microvessel area, defined in the microvessel area as a percentage of the total area in each field. In our study, there was a trend toward a positive correlation between %Signal intensity and %Vessel in meningioma, though it did not reach statistical significance, probably due to the small sample size. This finding was consistent with the results of Kimura et al. Weber et al⁹ attempted to elucidate the relationship between the average or maximal regional relative TBF on ASL-PI and the histopathologic findings, including the cell proliferation index, the microvessel area, and microvessel attenuation as defined by the number of microvessels.⁹ However, these comparisons yielded no significant correlations. They speculated that the lack of correlation might be attributable to the limitation of inherent sampling error associated with the high rate of stereotactic biopsy in their series (23/79 patients). In our study, only 1 patient was diagnosed by stereotactic biopsy, and the others were diagnosed by either surgical resection or open biopsy, which might have resulted in better histopathologic correlation with ASL-PI.

There are several indices for evaluating tumor vascular proliferation other than vascular attenuation, which was used

in this study. These include microvessel attenuation and size. Microvessel attenuation is well known as an indicator of the degree of malignancy in histopathologic studies of glioma,^{21,22} whereas microvessel area has also been reported as an indicator of malignant potential.²³ Exploration of the relationship between ASL-PI and those parameters of vascular proliferation is needed.

Among the gliomas, a statistically significant difference between high- and low-grade tumors was observed (Fig 4). Previous studies have shown that tumor blood volume, measured by dynamic susceptibility contrast MR perfusion imaging, provides useful information for assessing glioma grade.²⁹ More recently, it was reported that TBF measured by noninvasive ASL-PI could also be suitable for differentiating high-grade from low-grade gliomas.⁹⁻¹² Our result was in agreement with those reports. Given the positive correlation in our result between %Signal intensity and %Vessel in glioma, %Signal intensity could be an indicator of malignancy by depicting vascular attenuation. On the other hand, %Signal intensity positively correlated with the MIB1 index (Fig 3). However, it may be possible that the single data point of a very high MIB1 index mainly contributed to the positive correlation. Further studies to confirm this are needed.

This study has several limitations. The accuracy of blood

flow measurement was limited by a low signal intensity-to-noise ratio, which is inherent in ASL-PI.^{30,31} This could be serious, especially in the posterior fossa, where signal intensity loss can occur due to the susceptibility effect by the skull base bone. Low spatial resolution ($3.75 \times 3.75 \times 5$ mm) and limited section coverage (5 imaging sections of 3.5 cm of total width) were other technical limitations. The difference in feeding arteries (eg, internal carotid artery versus external carotid artery) may have affected the timing of the bolus arrival, possibly resulting in potential bias. There is a possible disagreement between the measurement region of signal intensity on ASL-PI and vascular attenuation on the histopathologic specimen. Further technical improvements and investigations with larger numbers of subjects are needed to confirm the results of our study.

Conclusion

Our results revealed a general positive correlation between %Signal intensity and %Vessel in brain tumors, suggesting that ASL-PI may predict the histopathologic vascular attenuation of brain tumors. ASL-PI may be useful in differentiating hemangioblastoma from other brain tumors and in distinguishing between high- and low-grade gliomas.

Acknowledgment

We thank Saori Uchida (Department of Neurosurgery, Kyushu University) for her helpful technical assistance.

References

- Chalela JA, Alsop DC, Gonzalez-Atavales JB, et al. **Magnetic resonance perfusion imaging in acute ischemic stroke using continuous arterial spin labeling.** *Stroke* 2000;31:680–87
- Kimura H, Kado H, Koshimoto Y, et al. **Multislice continuous arterial spin-labeled perfusion MRI in patients with chronic occlusive cerebrovascular disease: a correlative study with CO₂ PET validation.** *J Magn Reson Imaging* 2005;22:189–98
- Detre JA, Alsop DC, Vives LR, et al. **Noninvasive MRI evaluation of cerebral blood flow in cerebrovascular disease.** *Neurology* 1998;50:633–41
- Alsop DC, Detre JA, Grossman M. **Assessment of cerebral blood flow in Alzheimer's disease by spin-labeled magnetic resonance imaging.** *Ann Neurol* 2000;47:93–100
- Du AT, Jahng GH, Hayasaka S, et al. **Hypoperfusion in frontotemporal dementia and Alzheimer disease by arterial spin labeling MRI.** *Neurology* 2006;67:1215–20
- Liu HL, Kochunov P, Hou J, et al. **Perfusion-weighted imaging of interictal hypoperfusion in temporal lobe epilepsy using FAIR-HASTE: comparison with H₂15O PET measurements.** *Magn Reson Med* 2001;45:431–35
- Wolf RL, Alsop DC, Levy-Reis I, et al. **Detection of mesial temporal lobe hypoperfusion in patients with temporal lobe epilepsy by use of arterial spin labeled perfusion MR imaging.** *AJNR Am J Neuroradiol* 2001;22:1334–41
- Weber MA, Thilmann C, Lichy MP, et al. **Assessment of irradiated brain metastases by means of arterial spin-labeling and dynamic susceptibility-weighted contrast-enhanced perfusion MRI: initial results.** *Invest Radiol* 2004;39:277–87
- Weber MA, Zoubaa S, Schlieter M, et al. **Diagnostic performance of spectroscopic and perfusion MRI for distinction of brain tumors.** *Neurology* 2006;66:1899–906
- Warmuth C, Gunther M, Zimmer C. **Quantification of blood flow in brain tumors: comparison of arterial spin-labeling and dynamic susceptibility-weighted contrast-enhanced MR imaging.** *Radiology* 2003;228:523–32
- Wolf RL, Wang J, Wang S, et al. **Grading of CNS neoplasms using continuous arterial spin labeled perfusion MR imaging at 3 Tesla.** *J Magn Reson Imaging* 2005;22:475–82
- Gaa J, Warach S, Wen P, et al. **Noninvasive perfusion imaging of human brain tumors with EPISTAR.** *Eur Radiol* 1996;6:518–22
- Kimura H, Takeuchi H, Koshimoto Y, et al. **Perfusion imaging of meningioma by using continuous arterial spin-labeling: comparison with dynamic susceptibility-weighted contrast-enhanced MR images and histopathologic features.** *AJNR Am J Neuroradiol* 2006;27:85–93
- Louis DN, Ohgaki H, Wiestler OD, et al. **WHO Classification of Tumours of the Central Nervous System: Histological and Genetic Typing of Human Tumours.** Lyon, France: IARC PRESS; 2007
- Luh WM, Wong EC, Bandettini PA, et al. **QUIPSS II with thin-slice T1₁ periodic saturation: a method for improving accuracy of quantitative perfusion imaging using pulsed arterial spin labeling.** *Magn Reson Med* 1999;41:1246–54
- Noguchi T, Yoshiura T, Hiwatashi A, et al. **Quantitative perfusion imaging with pulsed arterial spin labeling: a phantom study.** *Magn Reson Med Sci* 2007;6:91–97
- Parkes LM, Tofts PS. **Improved accuracy of human cerebral blood perfusion measurements using arterial spin labeling: accounting for capillary water permeability.** *Magn Reson Med* 2002;48:27–41
- Parkes LM, Rashid W, Chard DT, et al. **Normal cerebral perfusion measurements using arterial spin labeling: reproducibility, stability, and age and gender effects.** *Magn Reson Med* 2004;51:736–43
- Donahue MJ, Lu H, Jones CK, et al. **An account of the discrepancy between MRI and PET cerebral blood flow measures: a high-field MRI investigation.** *NMR Biomed* 2006;19:1043–54
- Ye FQ, Berman KF, Ellmore T, et al. **H₂15O PET validation of steady-state arterial spin tagging cerebral blood flow measurements in humans.** *Magn Reson Med* 2000;44:450–56
- Abdulrauf SL, Edvardsen K, Ho KL, et al. **Vascular endothelial growth factor expression and vascular density as prognostic markers of survival in patients with low-grade astrocytoma.** *J Neurosurg* 1998;88:513–20
- Leon SP, Folkherth RD, Black PM. **Microvessel density is a prognostic indicator for patients with astroglial brain tumors.** *Cancer* 1996;77:362–72
- Korkolopoulou P, Patsouris E, Kavantzias N, et al. **Prognostic implications of microvessel morphometry in diffuse astrocytic neoplasms.** *Neuropathol Appl Neurobiol* 2002;28:57–66
- Gerdes J, Lemke H, Baisch H, et al. **Cell cycle analysis of a cell proliferation-associated human nuclear antigen defined by the monoclonal antibody Ki-67.** *J Immunol* 1984;133:1710–15
- Ellis PA, Makris A, Burton SA, et al. **Comparison of MIB-1 proliferation index with S-phase fraction in human breast carcinomas.** *Br J Cancer* 1996;73:640–43
- Cattoretto G, Becker MH, Key G, et al. **Monoclonal antibodies against recombinant parts of the Ki-67 antigen (MIB 1 and MIB 3) detect proliferating cells in microwave-processed formalin-fixed paraffin sections.** *J Pathol* 1992;168:357–63
- Burger PC, Shibata T, Kleihues P. **The use of the monoclonal antibody Ki-67 in the identification of proliferating cells: application to surgical neuropathology.** *Am J Surg Pathol* 1986;10:611–17
- Ho VB, Smirniotopoulos JG, Murphy FM, et al. **Radiologic-pathologic correlation: hemangioblastoma.** *AJNR Am J Neuroradiol* 1992;13:1343–52
- Aronen HJ, Gazit IE, Louis DN, et al. **Cerebral blood volume maps of gliomas: comparison with tumor grade and histologic findings.** *Radiology* 1994;191:41–51
- Wintermark M, Sesay M, Barbier E, et al. **Comparative overview of brain perfusion imaging techniques.** *J Neuroradiol* 2005;32:294–314
- Golay X, Hendrikse J, Lim TC. **Perfusion imaging using arterial spin labeling.** *Top Magn Reson Imaging* 2004;15:10–27